Available online at www.sciencedirect.com

SCIENCE DIRECT®

Journal of Molecular Catalysis A: Chemical 198 (2003) 303–308

JOURNAL OF MOLECULAR CATALYSIS A: CHEMICAL

www.elsevier.com/locate/molcata

Catalytic methanol decomposition over palladium deposited on thermally stable mesoporous titanium oxide

Mahendra P. Kapoor [a,1], Yuichi Ichihashi [a], Koji Kuraoka [a], Yasuyuki Matsumura [b,*]

[a] *National Institute of Advanced Industrial Science and Technology, Midorigaoka, Ikeda, Osaka 563-8577, Japan*
[b] *Research Institute of Innovative Technology for the Earth, Kizu-cho, Soraku-gun, Kyoto 619-0292, Japan*

Received 16 September 2002; accepted 9 December 2002

Abstract

Thermally stable mesoporous titanium oxide can be synthesized under non-aqueous conditions by reacting a sodium–glycotitanate(IV) complex and hexadecylamine in ethylene glycol. The mesoporous structure is retained after calcination in air at 350 °C for 5 h. Modification of the compound with palladium by the deposition–precipitation method results in formation of ultrafine palladium particles. Although a fairly large part of the particles are considered to be confined in the blind pores, the catalytic activity for methanol decomposition to carbon monoxide and hydrogen is significantly higher than that of palladium supported on a commercial titanium oxide.

Keywords: Mesoporous titanium oxide; Catalyst support; Palladium; Methanol decomposition; EXAFS

1. Introduction

Methanol decomposition to carbon monoxide and hydrogen has recently attracted a growing interest because the endothermic reaction is applicable to the energy recovery of the waste heat from a methanol-fuelled automobile in which the decomposition gas is supplied to the engine [1]. The heat recovery from industries is also possible, while new catalysts being active at low temperatures below 200 °C are required [2]. Palladium is active to the reaction especially when the support is zirconium oxide and cerium oxide on which palladium is highly dispersed [3–8]. Titanium oxide seems to be an active support, but the dispersion of palladium on the surface is not as high as on zirconium oxide and cerium oxide [4].

Silicic MCM-41 mesoporous materials have been often employed as a catalyst support and significant improvement in the activity was reported, probably because the catalytic metals can be highly dispersed in the characteristic pore structure with high surface area [9]. Mesoporous titanium oxide was first synthesized by Antonelli and Ying using a phosphate surfactant [10]. However, the structure is probably destroyed after the removal of the surfactant by a thermal treatment. Since thermal stability is usually required as a catalyst support, we have tried non-aqueous synthesis of mesoporous titanium oxide [11] and obtained the thermally stable product using hexadecylamine as a template [12].

Here we will show that the compound is an effective support of palladium which can be highly dispersed

* Corresponding author. Tel.: +81-774-75-2305; fax: +81-774-75-2318.
E-mail address: yasuyuki@rite.or.jp (Y. Matsumura).
[1] Present address: Toyota Central R&D Labs. Inc., Nagakute, Aichi 480-1192, Japan.

1381-1169/03/$ – see front matter © 2003 Elsevier Science B.V. All rights reserved.
doi:10.1016/S1381-1169(02)00732-X

in the pore structure by the deposition–precipitation method.

2. Experimental

Mesoporous titanium oxide was synthesized from sodium–glycotitanate(IV) complex prepared as described elsewhere [12]. Mixture of $Na_2Ti(C_2H_4O_2)_3 \cdot 4C_2H_6O_2$ complex (6.0 g) and hexadecylamine (1.8 g) was stirred in ethylene glycol (56 g), then NaOH (1.1 g) was added at 70 °C. The gel formed was heated at 80 °C for 4 days and cooled overnight. The compound was stirred in distilled water (300 g) for 6 h and left again for overnight to allow the formation of white precipitate which then sedimented. The solid was filtered and washed with distilled water, then dried in air at 100 °C for 1 day. Finally, it was calcined in air at 350 °C for 5 h.

Palladium was deposited onto the synthesized mesoporous titanium oxide or a commercial titanium oxide (P-25, Aero-sil) by a deposition–precipitation method [13]. The oxide was dispersed in a 0.01 M HCl aqueous solution of palladium chloride ($PdCl_2$, Kishida Chemicals), then palladium hydroxide was exclusively precipitated on the surface of the support by gradual addition of 1 M Na_2CO_3 aqueous solution to the palladium solution while heating to 70 °C and with continuously stirring the mixture. The pH of the solution was maintained at 10 for 1 h. The resulting solid was filtrated and washed with distilled water. The sample was dried at 120 °C overnight and calcined in air at 350 °C for 3 h.

Powder X-ray diffraction (XRD) patterns of the samples were recorded with a Rigaku Rotaflex 20 diffractometer using nickel-filtered Cu Kα. The pore size distribution was determined from the adsorption and desorption isotherm of nitrogen obtained with a BELSORP 28 (BEL Japan). The BET surface areas of the samples were determined from the isotherms of nitrogen physisorption.

Profiles of extended X-ray absorption fine structure (EXAFS) for the samples were taken at room temperature in transmission mode for K-edges of Pd at beam-line BL01B1 of SPring-8. The samples were reduced with hydrogen (0.02 MPa) at 300 °C for 1 h in a vacuum line and sealed with polyethylene films in a nitrogen atmosphere. The Fourier transformation was performed on k^3-weighted EXAFS oscillations in the range of 30–150 nm^{-1}. Normalization of the EXAFS function was done by dividing the absorption intensity by the height of the absorption edge. A cubic spline background subtraction was carried out. Inverse Fourier transform was obtained within the windows 0.19–0.57 nm in r space. The Pd–Pd reference was derived from the EXAFS of Pd foil. The analysis was performed with a program of "REX" supplied by Rigaku.

Catalytic reaction was performed in a fixed-bed continuous flow reactor under atmospheric pressure. A catalyst (0.20 g) diluted with 1.0 g of quartz sand being inert under the reaction conditions was sandwiched with quartz wool plugs in a quartz tube reactor of 6-mm i.d. The samples were reduced in a flow of 20 vol.% hydrogen diluted with argon (flow rate, 9.6 $dm^3\,h^{-1}$) for 1 h at 300 °C, then 20 vol.% of methanol was fed with an argon carrier (total flow rate 4.8 $dm^3\,h^{-1}$) at a desired temperature. The outlet gas was analyzed with an on-stream gas chromatograph (Yanagimoto G2800) equipped with a Porapak-T column (4 m) and a thermal conductivity detector. The activity test was reproducible within the error of 5%, when the total flow rate was 9.6 $dm^3\,h^{-1}$ with the same F/W.

Adsorption experiments were performed with a vacuum system equipped with Baratron vacuum gauges after the samples were reduced with hydrogen at 300 °C for 1 h.

X-ray photoelectron spectra (XPS) were recorded at room temperature with a Shimadzu ESCA 750. After reduction by hydrogen (20 kPa) at 300 °C for 1 h in a vacuum line, the well-ground sample was mounted in air onto a sample holder. In order to remove surface adsorbates, Ar-ion sputtering for 0.5 min at 2 kV and 20 mA was carried out just before the measurement. Binding energies were corrected by the reference of the C 1s line at 284.6 eV.

3. Results and discussion

3.1. Dispersion of palladium in mesoporous titanium oxide

In the X-ray diffraction pattern of the synthesized mesoporous titanium oxide (TiO_2-MS) there were

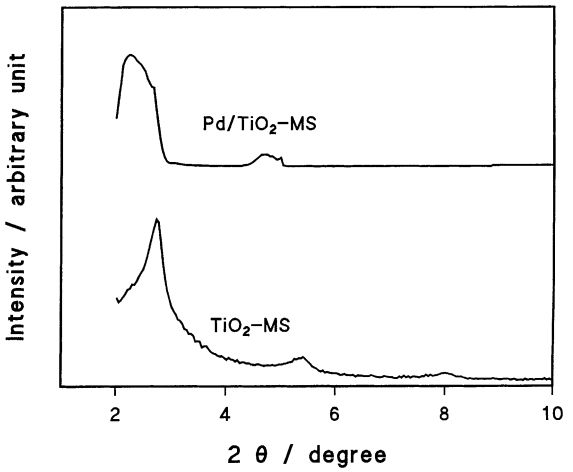

Fig. 1. XRD patterns of mesoporous titanium oxide and that modified with palladium by the deposition–precipitation method.

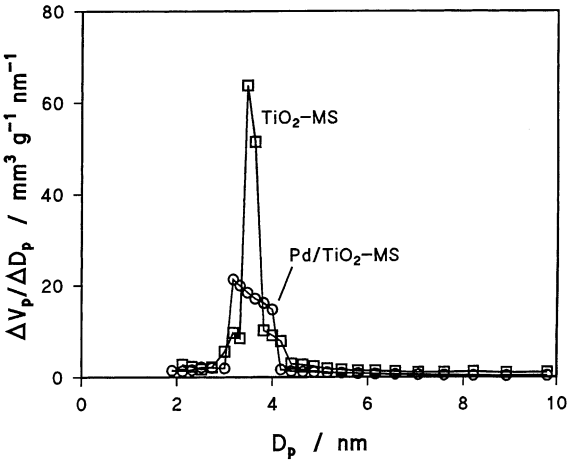

Fig. 2. Pore size distributions of mesoporous titanium oxide and that modified with palladium by the deposition–precipitation method. D_p, pore diameter; V_p, pore volume.

three peaks at 2.7, 5.4 and 8.0° in 2θ after calcination in air at 350 °C for 5 h (Fig. 1), showing successful synthesis of the stable titanium oxide with a mesoporous structure [10]. The peak at 2.7° can be indexed to a hexagonal lattice with d(1 0 0) spacing of 3.3 nm. We also prepared the mesoporous titanium oxide containing a phosphate surfactant according to the method reported by Antonelli and Ying [10], but the sample was unstable after the calcination at 350 °C.

The pore diameter of TiO_2-MS was sharply distributed at 3.5 nm with a pore volume of 74 $mm^3\,g^{-1}$ (Fig. 2). The distribution changed drastically after deposition of palladium. The pore diameter of the mesoporous compound containing 3 wt.% of palladium (Pd/TiO_2-MS) was widely distributed from 3.2 to 4.0 nm and the volume was reduced to 36 $mm^3\,g^{-1}$. The BET surface area was also reduced from 176 to 125 $m^2\,g^{-1}$. The change in the pore diameter was supported by the shift of the XRD peak originally at 2.7–2.3° in 2θ corresponding to 3.8-nm spacing (see Fig. 1) and the peak broadening is consistent with the wider distribution of the pore size. The peak intensity of the XRD for Pd/TiO_2-MS was similar to that for the parent material, suggesting that collapse of the pore scarcely takes place during the process of palladium loading although the pore volume and the BET surface area decreased significantly. The lack of the peak at 8.0° attributed to d(3 0 0) spacing shows loss of regular mesoscopic order in Pd/TiO_2-MS.

The Pd K-edge EXAFS spectrum of Pd/TiO_2-MS was compared with that of palladium (3 wt.%) supported on a commercial titanium oxide (Pd/TiO_2, 60 $m^2\,g^{-1}$). The Fourier transformation of the spectra show the presence of metallic Pd–Pd bonding at 0.24 nm (Fig. 3, phase shift uncorrected). The coordination number for the former sample was determined as 9.0 (Pd–Pd distance, 0.275 nm) which was significantly smaller than 10.6 (0.275 nm) for the latter (Table 1). The EXAFS parameters for the higher shells were not exact, but they were included in the calculation to increase the accuracy of the first-shell fitting. The calculated curve of k^3-weighted

Table 1
EXAFS parameters of Pd–Pd interaction for Pd/TiO_2-MS and Pd/TiO_2 reduced at 300 °C

Sample	Interatomic distance, r (nm)	Coordination number, n	Debye–Waller factor, σ (nm)
Pd foil	0.275	12.0	0.0060
	0.476	24.0	0.0060
	0.550	12.0	0.0062
Pd/TiO_2-MS	0.275	9.0	0.0070
	0.476	12.9	0.0071
	0.548	4.0	0.0067
Pd/TiO_2	0.275	10.6	0.0067
	0.478	21.6	0.0066
	0.544	9.1	0.0062

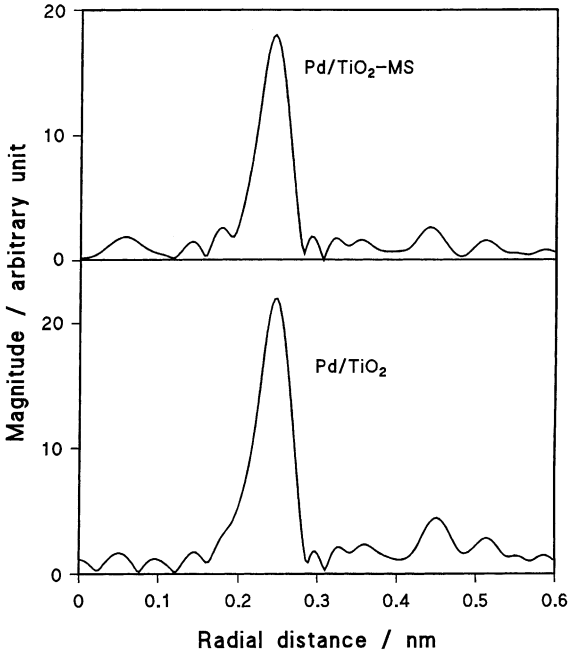

Fig. 3. Fourier-filtered Pd K-edge pseudoradial distribution functions of Pd/TiO_2-MS and Pd/TiO_2 reduced at 300 °C.

Pd K-edge EXAFS oscillations well fit the experimental data (Fig. 4). In the XRD pattern for Pd/TiO_2, the peak attributed to metallic palladium at 40.3° was present and the mean crystallite size was determined as 11 nm from the peak width using Sherrer's equation [14], but no such peak was observed in the pattern of Pd/TiO_2-MS. Prediction of particle size for metallic species from the EXAFS data has gained widespread use. The average particle size of palladium in Pd/TiO_2-MS can be estimated as 1–2 nm by the standard procedure proposed by Greegor and Lytle assuming spherical particles [15], while in their method the average coordination number is determined using geometrical shape models with face-centered-cubic (fcc) packing. Thus, palladium can be highly dispersed on the mesoporous titanium oxide.

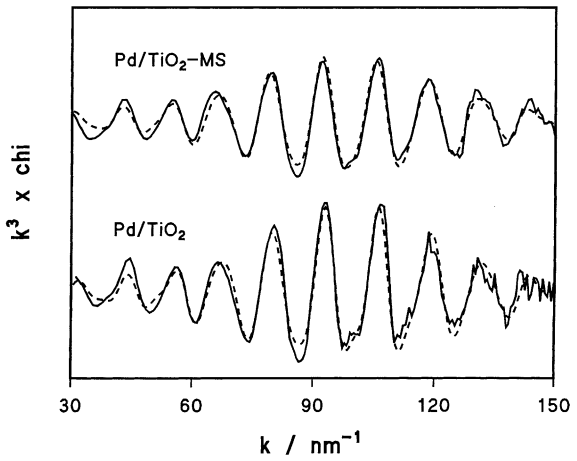

Fig. 4. k^3-Weighted Pd K-edge EXAFS oscillations for Pd/TiO_2-MS and Pd/TiO_2 reduced at 300 °C. Solid line, experimental data; broken line, calculated fit.

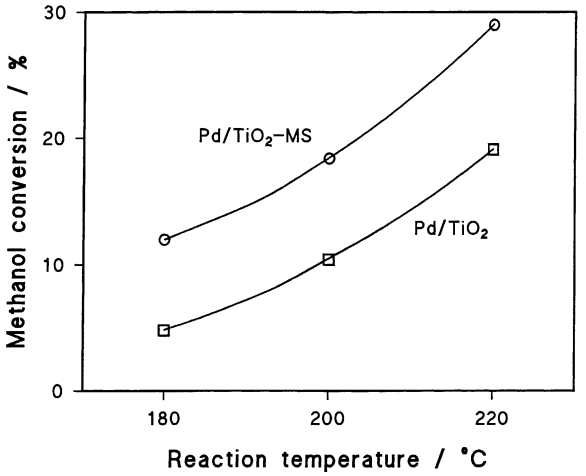

Fig. 5. Catalytic activity of Pd/TiO_2-MS and Pd/TiO_2 for methanol decomposition.

3.2. Catalytic activity for methanol decomposition

Methanol was selectively decomposed to carbon monoxide and hydrogen over the palladium catalysts. No byproduct such as methane was detected. The activity of Pd/TiO_2-MS at 180–220 °C was significantly higher than that for Pd/TiO_2, that is, the methanol conversions at 180 °C were 12.0 and 4.8%, respectively (Fig. 5).

Surprisingly, the palladium surface area for Pd/TiO_2-MS was 1.2 $m^2\,g^{-1}$ which was similar to that for Pd/TiO_2 (1.1 $m^2\,g^{-1}$). These values were calculated from the quantity of hydrogen strongly adsorbed on the surface (Fig. 6) assuming that hydrogen atoms are stoichiometrically adsorbed on palladium atoms whose site density is $1.3 \times 10^{19}\,m^{-2}$ [16].

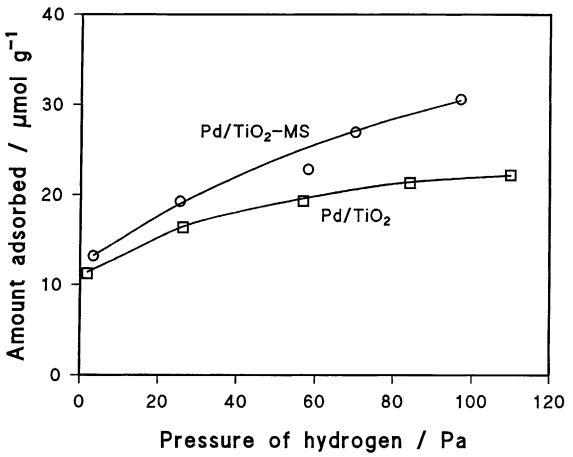

Fig. 6. Adsorption isotherms of hydrogen on Pd/TiO_2-MS and Pd/TiO_2 reduced at 300 °C.

The difference in the adsorption isotherm may be due to formation of palladium hydride phase in bulk [17]. The particle size of palladium in Pd/TiO_2 is calculated as 14 nm from the palladium surface area assuming spherical particles on the surface, and it is similar to the value estimated from the XRD measurement. However, the palladium area for Pd/TiO_2-MS is significantly smaller than the value of 7 $m^2\,g^{-1}$ expected from the particle size of 2 nm. Hence, a fairly large proportion of palladium particles in mesoporous titanium oxide are confined in blind pores which are probably choked with large palladium particles. The drastic decrease in the pore volume (see Fig. 2) without significant change in the XRD intensity (see Fig. 1) agrees with the presence of blind pores.

The catalytic activity at 180 °C did not increased so much as an increase in the palladium content of mesoporous titanium oxide (Fig. 7). Since the BET surface area decreased largely with an increase in the content, an increase in the palladium content is considered to result in an increase in the number of the blind pores. Thus, a significant portion of palladium is confined in the mesopores probably because the larger palladium particles are formed with the higher palladium content.

The turn-over frequency for Pd/TiO_2-MS at 180 °C is calculated as 0.60 s^{-1} on the basis of the palladium surface area which is double of that for Pd/TiO_2 (0.26 s^{-1}). It is known that cationic palladium species are active for methanol decomposition [3–8], and that these species are detectable from the XPS with a higher binding energy for Pd $3d_{5/2}$ than that for metallic palladium (335.0 eV) [18]. However, the binding energy for Pd/TiO_2-MS was 334.9 eV which is almost the same as that for Pd/TiO_2 (Fig. 8). The estimated error in the binding energy was ±0.2 eV. This indicated that the cationic palladium species are not formed in Pd/TiO_2-MS and the improvement in the catalytic activity is not due to the formation of a new species. This implies that the mesoporous structure affects the catalysis on palladium. Residual sodium ions would cause

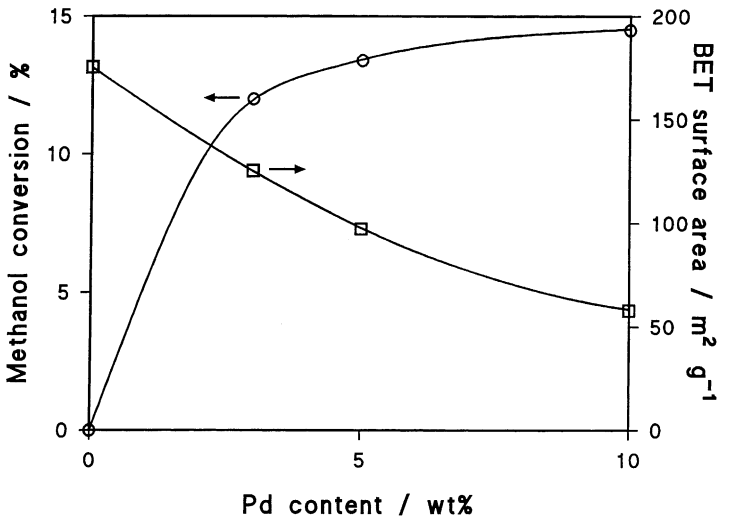

Fig. 7. Catalytic activity and the BET surface area of palladium supported on TiO_2-MS. Reaction temperature, 180 °C.

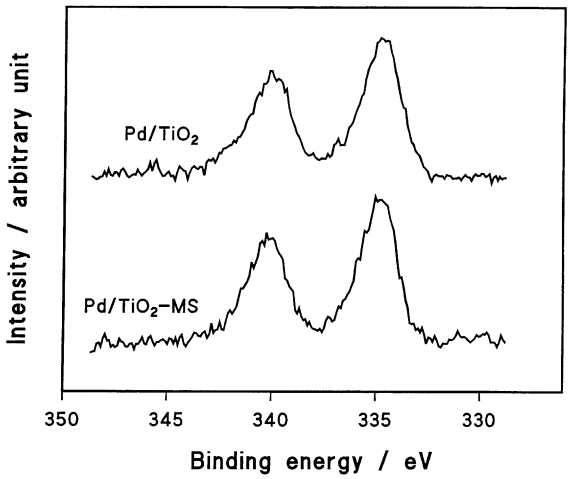

Fig. 8. XPS of Pd 3d region for Pd/TiO_2-MS and Pd/TiO_2 reduced at 300 °C.

the promotional effect, but no XPS peak attributed to Na 1s was observed in the spectra. The promotional effect of mesopores on the activity of palladium was found in the case of mesoporous zirconium oxide [19]. Since the walls of mesopores closely surround palladium particles, the concentration of methanol near palladium should increase by the interaction between the three-dimensional pores and methanol, and this may enhance decomposition of methanol. A similar effect was also observed with nickel supported on a porous glass, where the pore diameter of the porous glass was close to the nickel particles in the catalyst [20]. The interaction between the support and palladium would be strong in the mesopores, but no evidence was obtained in the XPS measurement.

It can be concluded that the mesoporous titanium oxide synthesized is stable and ultrafine palladium particles can be deposited on the oxide, probably because of the uniform pore structure which limits growth of the particles. Methanol decomposition is effectively catalyzed over palladium deposited on the mesoporous compound, although a fairly large proportion of the palladium particles are confined in the blind pores. The mesoporous structure may promote the reaction over palladium particles, however, further investigations are needed to confirm this.

Acknowledgements

The synchrotron radiation experiment was performed with the approval of the Japan Synchrotron Radiation Research Institute (Proposal 1999A0032-NX-np).

References

[1] Panel on New Directions in Catalytic Science and Technology, Board on Chemical Sciences and Technology, National Research Council, Catalysis Look to the Future, National Academy Press, Washington, DC, 1992.
[2] T. Nishimura, T. Omata, Y. Ogisu (Eds.), Eco-Energy City System, Energy Conservation Center, Tokyo, 1999 (in Japanese).
[3] Y. Matsumura, M. Okumura, Y. Usami, K. Kagawa, H. Yamashita, M. Anpo, M. Haruta, Catal. Lett. 44 (1977) 189.
[4] Y. Usami, K. Kagawa, M. Kawazoe, Y. Matsumura, H. Sakurai, M. Haruta, Appl. Catal. A 171 (1998) 123.
[5] Y. Usami, K. Kagawa, M. Kawazoe, Y. Matsumura, H. Sakurai, M. Haruta, Stud. Surf. Sci. Catal. 118 (1998) 83.
[6] Y. Matsumura, Y. Ichihashi, Y. Morisawa, M. Okumura, M. Haruta, Stud. Surf. Sci. Catal. 130 (2000) 2315.
[7] W.-J. Shen, Y. Matsumura, Phys. Chem. Chem. Phys. 2 (2000) 1519.
[8] W.-J. Shen, Y. Matsumura, J. Mol. Catal. A 153 (2000) 165.
[9] C.A. Koh, R. Nooney, S. Tahir, Catal. Lett. 47 (1997) 199 (the references therein).
[10] D.M. Antonelli, J.Y. Ying, Angew. Chem. Int. Ed. Engl. 34 (1995) 2014.
[11] D. Khushalani, G.A. Ozin, A. Kuperman, J. Mater. Chem. 9 (1999) 1491.
[12] G.J. Gainsford, T. Kemmitt, C. Lensink, N.B. Milestone, Inorg. Chem. 34 (1995) 746.
[13] W.-J. Shen, M. Okumura, Y. Matsumura, M. Haruta, Appl. Catal. A 213 (2001) 225.
[14] H.P. Klug, L.E. Alexander, X-ray Diffraction Procedures, Wiley, New York, 1954.
[15] R.B. Greeegor, F.W. Lytle, J. Catal. 63 (1980) 476.
[16] S.-Y. Wang, S.H. Moon, M.A. Vannice, J. Catal. 71 (1981) 167.
[17] J.A. McCaulley, J. Phys. Chem. 97 (1993) 10372.
[18] D. Briggs, M.P. Seah (Eds.), Practical Surface Analysis, second ed., vol. 1, Auger and X-ray Photoelectron Spectroscopy, Wiley, New York, 1990.
[19] M.P. Kapoor, Y. Ichihashi, W.-J. Shen, Y. Matsumura, Catal. Lett. 76 (2001) 139.
[20] Y. Matsumura, K. Kuraoka, T. Yazawa, M. Haruta, Catal. Today 45 (1998) 191.